JOC Article
pubs.acs.org/joc

Benzodifurantrione: A Stable Phenylogous Enol

Anthony J. Lawrence,*,† Michael G. Hutchings,*,† Alan R. Kennedy,‡ and Joseph J. W. McDouall§

†DyStarUK Ltd., School of Chemistry, University of Manchester, Manchester M13 9PL, U.K., ‡Department of Pure and Applied Chemistry, University of Strathclyde, Glasgow G1 1XL, U.K., and §School of Chemistry, University of Manchester, Manchester M13 9PL, U.K.

anthony.lawrence@manchester.ac.uk; mike.hutchings@manchester.ac.uk

Received October 15, 2009

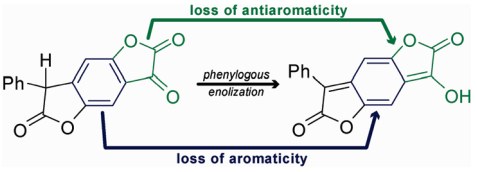

The first example of a stable phenylogous enol, resulting from an extended keto−enol tautomerization across a benzene ring, is described. The enol has been isolated, and its structure was proven by X-ray crystallography. The equilibrium between the keto- and enol-tautomers has been extensively studied and quantified in solution by NMR and UV−vis spectroscopy. The position of equilibrium showed a linear correlation to the Kamlet−Taft solvatochromic scale for solvent H-bond acceptor strength (β_{OH}), and the equilibrium was proven to be fully dynamic, obeying first-order equilibrium kinetics. To attempt to explain why enolization occurs, at what surprisingly appears to be the expense of aromatic resonance stabilization, various structural features have been considered and explored further with the aid of MO calculations. Nucleus independent chemical shift (NICS) index of aromaticity calculations for each of the rings comprising both tautomers showed that while the central benzene ring loses aromaticity on enolization, the α-keto-lactone ring showed an unexpected and significant *anti*aromaticity in the keto-tautomer, which is by no means intuitive. The loss of stabilization energy associated with the central benzene ring is, therefore, to a certain degree compensated by removal of the antiaromatic destabilization of the α-keto-lactone ring rendering the two structures much closer in energy than would otherwise be expected.

Introduction

The equilibrium between keto- and enol-tautomers for simple carbonyl compounds is normally strongly biased toward the more thermodynamically stable keto form.[1,2] As such, much research has been targeted at the study of the elusive enol entity, and its equilibrium with its keto-tautomer has been a prime topic of study in organic chemistry for many years.[1,3] In non-stabilized systems, the so-called "simple enols" of which vinyl alcohol is the simplest,[4] methods have been developed to synthesize the enols directly.[3a,5,6] Although thermodynamically unstable, many have sufficient kinetic stability in certain media to have allowed their structures to be studied extensively.[3b,c,5,7] Stabilized enol systems, such as 1,3-dicarbonyl,[3d,8,9] 1,5-dicarbonyl,[10−13] α-nitro, α-cyano,

(1) Toullec, J. *Adv. Phys. Org. Chem.* **1982**, *18*, 1–77.
(2) Keeffe, J. R.; Kresge, A. J.; Schepp, N. P. *J. Am. Chem. Soc.* **1988**, *110*, 1993–1995.
(3) Rappoport, Z. *The Chemistry of Enols* (*Chemistry of Functional Groups Series*); John Wiley & Sons Ltd: Chichester, 1990. (a) Chapters 5 and 8 of this book. (b) Chapters 4 and 8 of this book. (c) Stable "simple enols" are reviewed extensively in Chapter 8, parts C and D of this book. (d) Chapter 6, pp 353−378 of this book. (e) Chapter 4 of this book. (f) Aliphatic and alicyclic α-dicarbonyls are reviewed in Chapter 6, part V, pp 378−380 of this book.
(4) Hart, H. *Chem. Rev.* **1979**, *79*, 515–528.
(5) (a) Capon, B.; Zucco, C. *J. Am. Chem. Soc.* **1982**, *104*, 7567–7572. (b) Capon, B.; Rycroft, D. S.; Watson, T. W.; Zucco, C. *J. Am. Chem. Soc.* **1981**, *103*, 1761–1765.
(6) Capon, B; Siddhanta, A. K.; Zucco, C. *J. Org. Chem.* **1985**, *50*, 3580–3584.
(7) Capon, B; Siddhanta, A. K. *J. Org. Chem.* **1984**, *49*, 255–257.
(8) Forsén, S.; Nilsson, M. In *The Chemistry of the Carbonyl Group* (*Chemistry of Functional Groups Series*); Zabicky, J., Ed; Interscience-Wiley: London, 1970; Vol. 2, pp 198−226.
(9) Hesse, G. In *Methoden der Organischen Chemie* (*Houben-Weyl*); Müller, E., Bayer, O., Eds.; Thieme: Stuttgart, 1978; Vol. 6−1d; pp 9−216.
(10) Fuson, R. C.; Melby, L. R. *J. Am. Chem. Soc.* **1953**, *75*, 5402–5405.
(11) Bayly, R. C.; Barbour, M. G. In *Microbiological Degradation of Organic Compounds*; Gibson, D. T., Ed.; Marcel Dekker: New York, 1984; pp 253−294.
(12) Whitman, C. P.; Aird, B. A.; Gillespie, W. R.; Stolowich, N. J. *J. Am. Chem. Soc.* **1991**, *113*, 3154–3162.

Published on Web 01/07/2010 DOI: 10.1021/jo9022155

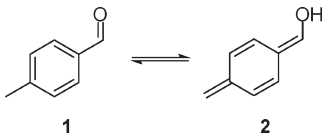

FIGURE 1. Implied phenylogous enolization across an aromatic ring.

α-acyl, α-phosphonyl, and α-sulfonyl carbonyl compounds,[8,9] are well-known. In these cases, the existence of at least one canonical resonance form for the enol-tautomer renders its energy more similar to or even lower than that for the keto-tautomer.[14] In addition, particularly in 1,3-dicarbonyl systems, an intramolecular H-bond between the enolic hydroxyl and the carbonyl function can add further stabilization to the enol-tautomer, especially in non-H-bonding solvents.[3d]

Although several examples exist for simple and stabilized enols, to date, we believe there to be no examples of stable extended phenylogous enols, i.e., enolization through an aromatic ring to give a hydroxyquinone dimethide as implied by **1** ⇆ **2** in Figure 1. Although such a process is theoretically feasible, clearly the enol-quinonoid form **2** lacks the aromatic resonance stabilization of the keto-benzenoid form **1**, which would be expected to render such an enol much higher in energy and hence thermodynamically unstable. Therefore, an absence of stable examples is not too surprising.

Hydroxyquinone dimethides, i.e., **2**, have been proposed as short-lived intermediates in bioactivation pathways,[15] *inter alia* in the biochemical (and chemical) reduction of anthracycline anticancer drugs.[16−18] One example, shown in Figure 2, is the tautomer **4** of 7-deoxydaunomycinone **5**, derived from the drug daunomycin **3** by reduction and elimination.[16a−c] However, *enolization* in these cases across a benzene ring to form a quinone dimethide (**2**) itself has not been observed. The enolic intermediates have been formed indirectly from reduction and elimination and convert rapidly to their thermodynamically more stable keto-benzenoid tautomers.

7-Phenyl-7*H*-benzo[1,2-b;4,5-*b*′]difuran-2,3,6-trione **6a**, known trivially as benzodifurantrione or BDT, is a molecule

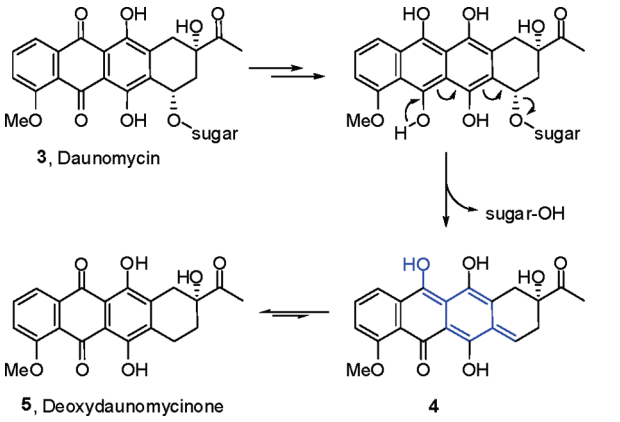

FIGURE 2. Proposed generation of a transient phenylogous enol by reduction of an anthracycline anticancer drug, exemplified with daunomycin **3**.[16]

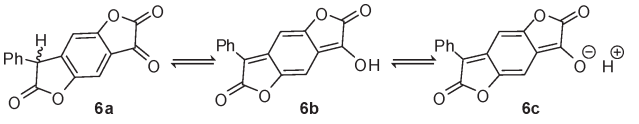

FIGURE 3. Proposed solvent-dependent phenylogous keto−enol tautomerization and enolate formation of BDT **6a**−**c**.

that has been of interest to us for some time, not least as a versatile intermediate to commercial benzodifuranone dyes.[19] Early attempts at structural analyses showed BDT **6a** to be more complex than would be expected, where it appeared to exist in different solvent-dependent forms.[19b] For example, in toluene or CH_2Cl_2, BDT gave a pale yellow solution that turned brownish red on standing, whereas in basic and/or H-bonding milieu such as DMF or DMSO, BDT gave an intense purple solution. These profound color differences led to the postulate that keto-BDT **6a** may in fact undergo this unusual form of phenylogous tautomerism allowing it to exist to a greater or lesser extent as the extended enol-quinonoid tautomer **6b** and/or enolate **6c**, without the use of strong base or the need for its generation from a precursor (Figure 3). However, given the absence of examples of this phenomenon in the literature, we remained unconvinced.

In this article, we now show that BDT is indeed the first example of a stable phenylogous enol. The enol has been isolated, and its structure was proven by X-ray crystallography. The equilibrium between the keto- and enol-tautomers has been studied and quantified in solution and proven to be fully dynamic. We also attempt to explain why BDT is such a special case, allowing enolization to occur, at what appears at first to be loss of aromatic stabilization.

Results and Discussion

BDT in the Solid State. BDT is highly pigment-like and shows limited solubility in many solvents. However, suitable single crystals were grown from methyl-isobutyl ketone to allow X-ray structure analysis. Figure 4a shows the contents of the asymmetric unit, in which two independent conformers

(13) Lam, W. W. Y.; Bugg, T. D. H. *J. Chem. Soc., Chem. Commun.* **1994**, 1163–1164.
(14) Waring, A. L. In *Comprehensive Organic Chemistry*; Stoddart, J. F., Ed.; Pergamon: Oxford, 1979; Vol. 1, pp 1024−1026.
(15) (a) Moore, H. W. *Science* **1977**, *197*, 527–532. (b) Moore, H. W.; Czerniak, R. *Med. Res. Rev.* **1981**, *1*, 249–280.
(16) (a) Kleyer, D. L.; Koch, T. H. *J. Am. Chem. Soc.* **1984**, *106*, 2380–2387. (b) Kleyer, D. L.; Koch, T. H. *J. Am. Chem. Soc.* **1983**, *105*, 2504–2505. (c) Boldt, M.; Gaudiano, G.; Koch, T. H. *J. Org. Chem.* **1987**, *52*, 2146–2153. (d) Gaudiano, G.; Frigerio, M.; Sangsurasak, C.; Pierfrancesco, B.; Koch, T. H. *J. Am. Chem. Soc.* **1992**, *114*, 5546–5553. (e) Gaudiano, G.; Frigerio, M.; Pierfrancesco, B.; Koch, T. H. *J. Am. Chem. Soc.* **1992**, *114*, 3107–3113. (f) Schweitzer, B. A.; Egholm, M.; Koch, T. H. *J. Am. Chem. Soc.* **1992**, *114*, 242–248. (g) Gaudiano, G.; Koch, T. H. *J. Am. Chem. Soc.* **1990**, *112*, 9423–9425. (h) Bird, D. M.; Boldt, M.; Koch, T. H. *J. Am. Chem. Soc.* **1989**, *111*, 1148–1150. (i) Kleyer, D. L.; Gaudiano, G.; Koch, T. H. *J. Am. Chem. Soc.* **1984**, *106*, 1105–1109.
(17) Kleyer, D. L.; Koch, T. H. *J. Am. Chem. Soc.* **1983**, *105*, 5154–5155.
(18) (a) Ramakrishnan, K.; Fischer, J. *J. Med. Chem.* **1986**, *29*, 1215–1221. (b) Ramakrishnan, K.; Fischer, J. *J. Am. Chem. Soc.* **1983**, *105*, 7187–7188. (c) Gaudiano, G.; Resing, K.; Koch, T. H. *J. Am. Chem. Soc.* **1994**, *116*, 6537–6444. (d) Bird, D. M.; Gaudiano, G.; Koch, T. H. *J. Am. Chem. Soc.* **1991**, *113*, 308–315. (e) Gaudiano, G.; Frigerio, M.; Pierfrancesco, B.; Koch, T. H. *J. Am. Chem. Soc.* **1990**, *112*, 6704–6709. (f) Gaudiano, G.; Egholm, M.; Haddadin, M. J.; Koch, T. H. *J. Org. Chem.* **1989**, *54*, 5090–5093. (g) Egholm, M.; Koch, T. H. *J. Am. Chem. Soc.* **1989**, *111*, 8291–8293. (h) Boldt, M.; Gaudiano, G.; Haddadin, M. J.; Koch, T. H. *J. Am. Chem. Soc.* **1989**, *111*, 2283–2292.

(19) (a) Hughes, N.; Newton, D. F.; Milner, D. J.; Deboos, G. A. World Patent WO 94/12501. (b) James, M.; Bradbury, R. World Patent WO 95/28447.

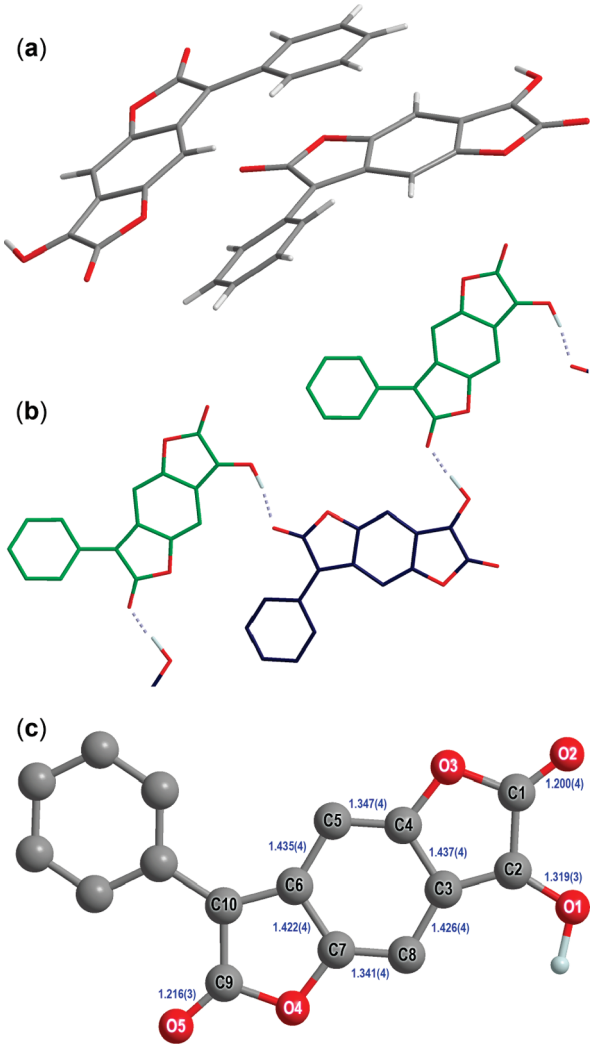

FIGURE 4. (a) Asymmetric unit showing two independent conformers, both enol structures **6b**, differing in the twist angles (13.3(2)° and 24.9(2)°) of the *exo*-7-phenyl ring. (b) Intermolecular H-bonding observed between the two conformers displayed in green and blue. (c) Atom labels and key bond lengths (Å; in blue) for one conformer (13.3(2)° twist).

were observed; Figure 4b shows the intermolecular hydrogen bonding, and Figure 4c shows the important bond lengths in one of the conformers. The conformers differed only by the twist angle of the 7-phenyl ring, which was 13.3(2)° and 24.9(2)° in each case (as defined by the dihedral angle between the least-squares planes of the phenyl rings and the five-membered rings to which they are attached). In the crystal structure, both conformers exist as the enol-tautomer **6b**. The central ring is clearly quinonoid rather than benzenoid with the bond lengths of the formal C=C double bonds (C4−C5, C7−C8) in the central ring being shorter (1.347(4), 1.341(4) Å) than the formal single bonds (1.426(4)−1.442(4) Å). The H-atom is found on the enolic OH group (O1) and the benzylic carbon (C10) is sp^2 hybridized with the three bond angles at these centers totaling 360.0°. Rather than adopt an intramolecular five-membered H-bond between the enol

(20) Shimanouchi, H.; Sasada, Y. *Acta Crystallogr., Sect. B* **1973**, *29*, 81–90.

SCHEME 1. Synthesis of Locked Enol-Ether 7, α-Keto-Ester 8, and α-Keto-Acid 9

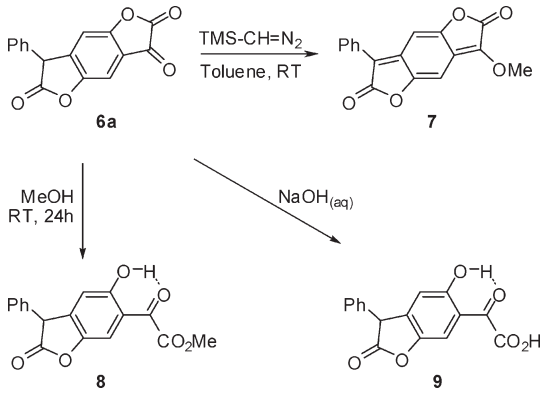

hydroxyl and adjacent lactone carbonyl or exist as dimers as is found for tropolone-type structures,[20] the molecules form intermolecular H-bonded chains between the enol OH (O1) of one conformer and the carbonyl oxygen (O5) of the opposite lactone ring of the other conformer.

IR analysis of BDT in the solid state (KBr) also supported the enol-tautomer **6b**. Absorbances at 1782 and 1692 cm^{-1} were observed for the two lactones; the higher frequency of one of the lactone stretches is explicable due to H-bonding to the enolic OH, as seen in the crystal structure. Further absorbances at 1623 and 1579 cm^{-1} were also evident and appear to be characteristic of the double bonds of the quinone dimethide.

BDT in Solution; Keto/Enol Standards. In parallel with the solid-state investigations, we looked in depth at the behavior of BDT in solution by NMR and UV−vis spectroscopy. To aid investigation, enol-locked analogue **7** was prepared by treating **6a** in toluene with TMS-diazomethane (Scheme 1).[21] All analytical data were consistent with the proposed structure **7**.

The IR spectrum (KBr) was similar to that for BDT-enol **6b** above. Absorption bands were observed at 1785 and 1753 cm^{-1} for the two lactones and at 1620 and 1583 cm^{-1} for the quinone dimethide. In this case, both lactone stretches had a similar frequency since no intermolecular H-bonding exists, unlike for BDT-enol **6b**.

The ^1H NMR spectrum (CD_3CN, Figure 5a) showed no benzylic proton resonance and showed the methyl group as a 3-proton singlet at δ 4.33 ppm, indicating that it was O- rather than C-linked. The two central ring proton resonances were seen at δ 6.97 and δ 6.93 ppm, and the two *ortho*-protons of the 7-phenyl ring appeared at δ 7.75 ppm. The relatively high-field shifts for the central ring protons are comparable to the shifts seen for 1,4-benzoquinone (δ 6.76 ppm).[22] The upfield shifts for these central ring protons and the relatively low-field shift for the 7-phenyl *ortho*-protons proved to be extremely characteristic of the enol-quinonoid form. ^{13}C NMR showed the two lactone resonances at δ 168.0 and δ 162.2 ppm, and no lower field ketone resonance was observed. Instead, the derived C=*C*-OMe enolic carbon was observed at δ 145.1 ppm, displaying a strong correlation in an HMBC experiment to

(21) Coe, D.; Drysdale, M.; Philps, O.; West, R.; Young, D. W. *J. Chem. Soc., Perkin Trans. 1* **2002**, 2459–2472.

(22) Tamura, Y.; Yakura, T.; Tohma, H.; Kikuchi, K.; Kita, Y. *Synthesis* **1989**, 126−127, compound **3c**.

the OCH_3 enol ether carbon, which itself resonated at δ 60.8 ppm. The two central quinonoid ring methine carbon resonances were also highly distinctive, observed almost coalesced at δ 97.97 and δ 98.00 ppm.

UV−vis spectra of **7** were measured in numerous solvents, and the extinction coefficients were calculated. Compound **7** displayed modest solvatochromism, which was ascribed to solvent polarizability,[23] with extremes of λ_{max} 432 nm (MeCN) and λ_{max} 446 nm (*o*-dichlorobenzene) for the solvents studied. To normalize for varying absorbance peak shape across the studied solvents, the extinction coefficients were multiplied by the fwhm (full width at half maximum) to give the approximate peak area ($\varepsilon \times$ fwhm).[24] Full results are detailed in Table 1. With the exception of THF and 2-propanol, the $\varepsilon \times$ fwhm values were relatively consistent across all solvents studied, with an average of 2.96×10^6 (range, $2.81 \times 10^6 - 3.10 \times 10^6$). The values provided for THF and 2-propanol are averages over five measurements. In THF compound **7** gave a cloudy solution, and it was highly insoluble in 2-propanol, leading to difficulties in accurate measurement and explaining the outlying results. These two solvents were thus omitted in calculating the average $\varepsilon \times$ fwhm value.

During UV−vis analysis (below), it was observed that dissolution of BDT **6a** in methanol led to ring opening to give α-keto-methyl ester **8**. A standard of **8** was prepared by stirring for 24 h at room temperature in methanol. The acquired ^{1}H NMR spectrum (Figure 5b) was fully consistent with **8** existing solely as the keto-benzenoid tautomer in all deuterated solvents other than DMSO-d_6, and as such served as a useful keto-tautomer NMR standard. In CD_3CN, the benzylic proton resonated at δ 5.15 ppm, the two central ring protons at δ 6.91 and δ 7.61 ppm, and in this case the *ortho*-protons of the 7-phenyl ring appeared upfield at δ 7.26 ppm. The distinctive differences in the shifts of the central ring and 7-phenyl ring *ortho*-protons in the ring-opened α-keto-ester **8** are notable compared with enol-ether **7**. IR data in the solid state showed absorbances at 1791 cm^{-1} for the β,γ-unsaturated lactone, 1741 cm^{-1} for the ester, and 1624 cm^{-1} for the intramolecularly H-bonded aryl ketone. A single absorbance was seen in the UV region at λ_{max} 368 nm with ε_{max} of 4,250 and fwhm of 62 nm.

BDT in Solution; NMR Studies. ^{1}H NMR studies of BDT were conducted in CD_3CO_2D and in a range of other deuterated solvents containing a trace of methane sulfonic acid (MSA) to determine the keto/enol constitution. The inclusion of MSA was required to remove any ionized-BDT **6c** from the equilibrium (see UV−vis studies below); omission of MSA gave broad spectra with multiple species. All solutions were heated to ca. 100 °C or boiling (depending on solvent boiling point) to ensure equilibrium was achieved from the solid-state constitution. The peaks were sharp and well resolved indicating that keto−enol exchange was slow on the ^{1}H NMR time scale at ambient temperature. In all cases both keto- and enol-tautomers were observed, and the tautomer ratios were calculated from integration of the spectra.

(23) Catalán, J.; Hopf, H. *Eur. J. Org. Chem.* **2004**, 4694–4702.

(24) We use the $\varepsilon \times$ fwhm area approximation rather than ε', the exact area derived extinction coefficient, since the true area could not be measured due to the overlap of the keto (**6a**) absorbance (λ_{max} ca. 295 nm) with the hypsochromic tail of the enol (**6b**) absorbance and with solvent absorption in some cases (e.g., acetone) despite the use of a blank balancing cell.

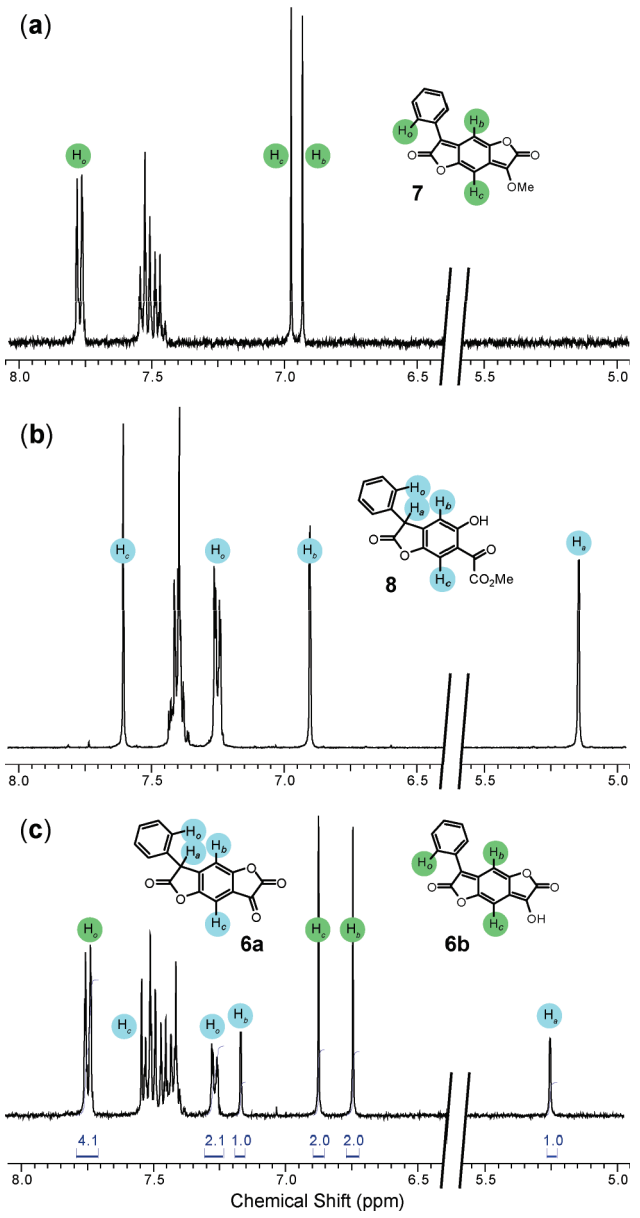

FIGURE 5. ^{1}H NMR (CD_3CN) key resonances for (a) locked enol-tautomer **7**, (b) keto-tautomer standard **8**, (c) BDT showing 1:2 [keto **6a**]:[enol **6b**] ratio from integration.

As an example, Figure 5c shows the ^{1}H NMR spectrum for BDT in CD_3CN compared to locked enol-tautomer **7** (Figure 5a) and keto-standard **8** (Figure 5b). Both tautomers are clearly visible with a [keto]:[enol] ratio of 1:2 by integration. For the BDT keto-tautomer **6a**, the diagnostic protons resonate at δ 5.23 ppm (H_a), δ 7.17 ppm (H_b), δ 7.27 ppm (H_o), and δ 7.56 ppm (H_c), which are consistent with the respective shifts of the protons in the keto-standard **8** at δ 5.17 ppm (H_a), δ 6.95 ppm (H_b), δ 7.23 ppm (H_o), and δ 7.58 ppm (H_c). Likewise, the diagnostic protons for the enol-tautomer **6b** resonate at δ 6.75 ppm (H_b), δ 6.87 ppm (H_c) and δ 7.75 ppm (H_o), again consistent with the respective shifts of the protons in the enol-standard **7** at δ 6.93 ppm (H_b), δ 6.97 ppm (H_c) and δ 7.75 ppm (H_o). Results of keto/enol ratios for BDT calculated from ^{1}H NMR spectra in other solvents studied are summarized along with UV−vis data in the next section in Table 3.

TABLE 1. UV Data for Locked Enol-Tautomer 7 in a Variety of Solvents

solvent	λ_{max} (nm)	ε_{max} (M^{-1} cm^{-1})	fwhm[a] (nm)	$\varepsilon \times$ fwhm ($\times 10^6$)
acetic acid	434	37,250	79	2.94
acetone	433	39,250	78	3.06
acetonitrile	432	38,500	78	3.00
benzonitrile	444	39,250	79	3.10
chlorobenzene	444	39,250	78	3.06
chloroform	440	37,000	77	2.85
cyclohexane/toluene (90/10)	435	42,000	71	2.98
o-dichlorobenzene	446	36,500	78	2.85
dichloromethane	438	38,500	77	2.96
DMSO	445	35,750	84	3.00
1,4-dioxane	437	36,500	77	2.81
ethyl acetate	433	38,500	78	3.00
methyl isobutyl ketone	435	38,250	78	2.98
2-propanol[b]	435	$32,250 \pm 6000$	78	2.52 ± 0.46
THF[c]	436	33,250	80	2.66
toluene	443	37,000	77	2.85

[a]Full width at half maximum. [b]Sparingly soluble in this solvent; measured ε_{max} may be inaccurate. [c]Cloudy solution; measured ε_{max} may be inaccurate.

Obtaining clear ^{13}C NMR data for the BDT tautomeric mixture was problematic because of its low solubility. In solvents such as DMSO where solubility was good, BDT existed solely as its enolate **6c** (properties discussed below). In solvents offering lower but sufficient solubility, such as acetone, dioxane, or 2-propanol, the equilibrium was displaced too far toward the enol to resolve the keto resonances with certainty above the noise. In acetonitrile-d_3 (containing 33% of the keto-tautomer), signal-to-noise was just sufficient to observe all key carbon resonances for both tautomers (Table 2) with the exception of carbon C_g in both tautomers (as defined below), which were lost under the solvent nitrile peak. Assignments were made aided with HMQC analysis, by comparison to the enol-ether and keto-ester standards **7** and **8**, and by comparison to literature reported shifts for close analogue coumarandione (**10**; Figure 6).[25] Due to low BDT solubility, meaningful HMBC data could not be obtained to allow direct unambiguous assignment of all carbons. Therefore, assignment of those carbons without an HMQC correlation could only be inferred by comparison. The majority of resonances for the keto-tautomer **6a** were comparable to the keto-standard **8**. Of note are the benzylic methine carbon C_a at δ 52.0 ppm, lactone carbon C_j at δ 175.0 ppm, and the central benzene ring tertiary carbons C_c and C_h at δ 112.5 and δ 107.7 ppm. In this case, C_c was at lower field than C_h (determined from the HMQC data), unlike in the keto-standard **8**, in the enol-tautomer **6b**, and in the enol-ether **7**. The shifts for the ketone and lactone carbons C_f (δ 178.8 ppm) and C_e (δ 152.7 ppm) in the keto-tautomer **6a** were significantly upfield, cf. standard **8**. However, these shifts were consistent with those determined for the respective carbons of coumarandione at δ 177.1 and δ 155.9 ppm.[25] The further shielding of these carbons in the ring-closed α-keto-lactone tautomer of coumarandione **10** and BDT-keto **6a** compared to the ring-opened α-keto-ester **8** is consistent with antiaromatic character in this ring, a key point that is discussed in detail below.

(25) (a) Winkler, T.; Ferrini, P. G.; Haas, G. *Org. Magn. Reson.* **1979**, *12*, 101–102. (b) Galasso, V.; Pellizer, G.; Pappalardo, G. C. *Org. Magn. Reson.* **1980**, *13*, 228.

TABLE 2. Assignment of Key ^{13}C Resonances of BDT-Keto 6a and BDT-Enol 6b Tautomer Mixture in CD_3CN by Comparison to Keto-Ester 8 and Enol-Ether 7 Standards and to Literature-Reported Shifts for Coumarandione[25]

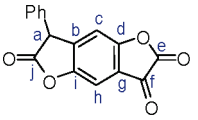

6a

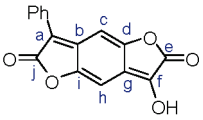

6b

carbon	δ_C ppm **6a**	δ_C ppm **8**[a]	δ_C ppm **6b**	δ_C ppm **7**[a]
a	52.0[b]	50.6	122.9	120.1
b	135.7	139.2	141.3	138.7
c	112.5[b]	106.6	97.4[b]	98.0
d	164.9[e]	159.0	152.0	149.8
e	152.7[c]	162.5	162.0[e]	162.2
f	178.8	188.8	144.3	145.1
g	117−120[d]	110.7	117−120[d]	116.6
h	107.7[b]	111.3	98.8[b]	98.0
i	142.4	146.5	155.5	153.5
j	175.0[c]	174.2	169.8	168.0

[a]Assigned by HMQC and HMBC analysis. [b]Assigned by HMQC. [c]Weak peak observable just above noise threshold. [d]Peak obscured by solvent CN resonance at 117−120 ppm. [e]Possible that these two peaks are inversely assigned.

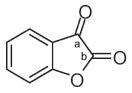

10 δ_C ($CDCl_3$) 177.1 (a), 155.9 (b)

FIGURE 6. Selected reported ^{13}C shifts for coumarandione **10**.[25a]

No evidence existed in the ^{13}C spectrum for the possible alternative ketone-hydrate structure. The chemical shifts for the enol-quinonoid tautomer **6b** were very similar to those observed for the locked enol-ether **7**. Those of note are the two tertiary central quinonoid ring carbons C_c and C_h at δ 97.4 and δ 98.8 ppm, the enol carbon C_f at δ 144.3 ppm, and the two lactone carbons C_e and C_j at δ 162.0 and δ 169.8 ppm.

BDT in Solution; UV−vis Studies. The UV−vis spectrum of BDT was measured in a range of solvents, and data are summarized in Table 3. Example spectra are reproduced in Figure 7. In DMSO and DMF, BDT gave a bright purple solution with a single absorbance in the visible region at 554 and 552 nm, respectively. In acetic acid, $CHCl_3$, and Cl_3CCO_2Et, a single absorption was seen in the visible region at 432 nm. In all other solvents both absorptions were observed at 425−444 and at 530−550 nm, the proportions of which shifted on standing in favor of the bathochromic 530−550 nm absorbance. Adding a trace amount of methane sulfonic acid (MSA) removed the 530−550 nm absorption from the spectrum for the solvents other than DMF and DMSO and left a dominant absorption at 425−444 nm. Knowing that locked enol-ether **7** had an average λ_{max} of 438 nm in the solvents studied, it followed that the absorption band seen for BDT at 425−444 nm in the same solvents was due to the electronically comparable enol-quinonoid tautomer **6b**. The absorption at ca. 550 nm, giving rise to the purple coloration, was explained by BDT being fully or partially ionized, i.e., as its extended enolate **6c**, which bears a stronger donor leading to a bathochromic shift. This form of BDT is discussed in more detail later in this article. In acidic media, such as in acetic acid or by adding a trace of

TABLE 3. UV−vis and ^{1}H NMR [keto 6a]:[enol 6b] Ratio Data Measured in Various Solvents Containing a Trace of MSA

solvent	HBA β_{OH}[a]	λ_{max} (nm)	ε_{max} (M^{-1} cm^{-1})	fwhm[b] (nm)	ε_{max} × fwhm (×10^6)	% enol by UV−vis[c]	% enol by NMR[d]	log K[e]	ΔG (kJ mol^{-1})
acetic acid[f]	0.45	433	31,250	81	2.53	86	90	0.954	−5.44
acetone	0.49	432	32,250	81	2.61	88	88	0.865	−4.94
acetonitrile	0.39	428	23,000	80	1.84	62	66	0.288	−1.63
anisole	0.21	441	15,500	82	1.27	43		−0.122	+0.71
benzonitrile	0.37	444	28,500	74	2.11	71		0.389	−2.22
chlorobenzene	0.07	436	11,500	82	0.94	32	25[g]	−0.327[g]	+1.88
chloroform[f,h]	0.10	431	(8,750)[h]	82	0.72	(24)[h]	40	−0.176	+1.00
o-dichlorobenzene	0.03	438	11,250	85	0.96	32	38	−0.213	+1.21
DMF[i]	0.73	552	35,000			exists as enolate			
dimethyl phthalate	0.41	440	26,250	81	2.13	72		0.410	−2.34
DMSO[i]	0.73	554	35,000			exists as enolate			
1,4-dioxane	0.46	435	32,500	78	2.54	86	88	0.865	−4.94
ethyl acetate	0.50	430	30,250	79	2.39	81		0.630	−3.56
ethyl trichloroacetate[f]	0.25	433	16,250	84	1.37	46		−0.070	+0.42
methyl isobutyl ketone	0.48	433	33,500	80	2.68	91		1.005	−5.73
2-propanol	0.84	439	33,500	87	2.91	99	99.5	2.299	−13.1
tetrahydrofuran	0.59	436	34,750	85	2.95	100	95.5	1.33	−7.53
toluene	0.10	437	11,500	83	0.96	32		−0.327	+1.88

[a]Kamlet−Taft solvatochromic scale of H-bond acceptor strength (β_{OH}).[33] [b]Full width at half maximum. [c]% Enol calculated from ($\varepsilon_{max\mathbf{6b}}$ × $fwhm_{\mathbf{6b}}$)/ 2.96 × 10^6 (2.96 × 10^6 is the average ε_{max} × fwhm for enol-ether **7** from Table 1). [d]% Enol calculated from comparison of averaged keto/enol integrals in the ^{1}H NMR spectrum where measured. [e]log *K* based on NMR enol content where available, otherwise calculated from UV−vis estimates. [f]MSA omitted due to intrinsic solvent acidity. [g]log K based on UV due to broad NMR spectrum. [h]BDT highly insoluble in this solvent; measured ε_{max} may be inaccurate. [i]MSA omitted; BDT existed as enolate and could not be fully protonated in this solvent.

MSA to the solvents (excluding DMF and DMSO), BDT existed fully protonated and the 550 nm absorption disappeared,[26] whereas addition of a trace of Et_3N gave a full shift to the 550 nm absorption.

The keto-benzenoid tautomer **6a** was observed between 292 and 300 nm for solutions of BDT in solvents transparent to relatively high energies and which supported high keto contents. Treatment with solvents that favored enol-tautomer formation (e.g., 2-propanol) eliminated the ca. 300 nm band assigned to keto-BDT **6a**, and the intensity of enol absorption at ca. 430 nm correspondingly increased (Figure 7).[27]

After removing the enolate **6c** by addition of MSA, the observed solvent dependency of the extinction coefficients for the ca. 430 nm absorption was directly related to the proportion of enol-quinonoid in that solvent at equilibrium. The absorbance for **6b** in acidified media showed a linear relationship when plotted versus concentration, demonstrating that the keto:enol equilibrium was not perturbed by concentration over the range studied.[28] Knowing that the average value of ε × fwhm for enol-ether **7** was 2.96 × 10^6 in the solvents studied, it was possible to use this measurement to estimate the [keto]:[enol] ratio for BDT at equilibrium by comparison, e.g., ($\varepsilon_{max\mathbf{6b}}$ × $fwhm_{\mathbf{6b}}$)/2.96 × 10^6.[29] This assumed that the enol **6b** had an extinction coefficient equal to that for the enol-ether **7**, which is not necessarily always the case.[30] However, in this instance, this assumption gave

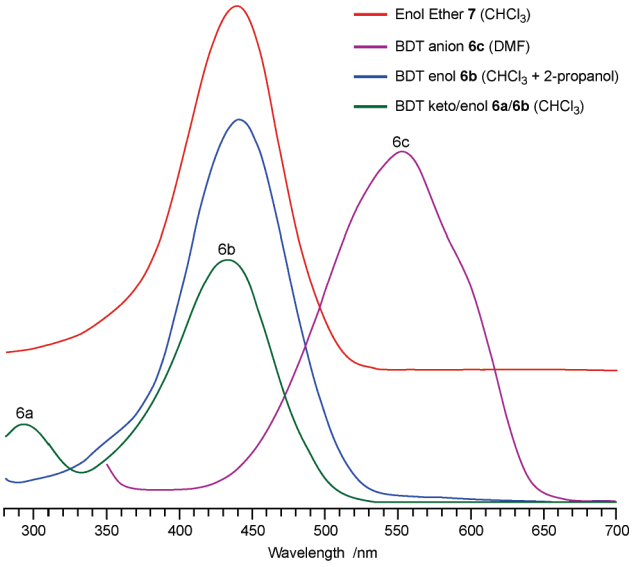

FIGURE 7. Selected UV−vis spectra for BDT (**6a**−**c**) and enol-ether **7** in various media. Spectra for BDT in $CHCl_3$ with and without 2-propanol were measured at identical concentration.

figures consistent with the ratios observed by NMR in the same solvents and thus served as a useful and simple method to estimate the enol-quinonoid **6b** content.[31] The calculated [keto]:[enol] ratios are given in Table 3 with comparison to the observed NMR ratios where measured. In all cases, the solutions were prepared using solvents with < 50 ppm water content and by heating to ca. 100 °C or boiling to ensure equilibrium was reached. Solutions in relatively water-immiscible solvents, such as chlorobenzene, showed little change in ε_{max} on standing overnight. In other water-miscible solvents, a slow decline in ε_{max} over time was observed (ca. 10−20% overnight), which was attributed to the slow hydrolysis of the α-keto-lactone to the ring-opened α-keto-acid **9**. This was confirmed experimentally by leaving a 10% water/dioxane solution of BDT containing a trace of MSA to

(26) Presumably the commercially obtained chloroform and ethyl chloroacetate used for the UV−vis studies contained sufficient residual acid to protonate dissolved enolate without the requirement of additional MSA.

(27) The keto (**6a**) UV assignment is discussed further in Supporting Information.

(28) One example in acetone is supplied in Supporting Information.

(29) Further notes on the selection of ε × fwhm for enol quantification by UV−vis are available in Supporting Information.

(30) Rhoads, S. J.; Pryde, C. *J. Org. Chem.* **1965**, *30*, 3212–3214.

(31) Accuracy of measurements by UV−vis was probably less than by NMR. When UV−vis spectra were run in triplicate, around 5% variation was found in the calculated enol content. In addition, slight perturbations from the averaged value for ε × fwhm of 2.96 × 10^6 for the enol-ether **7** in each specific solvent may have existed.

stand overnight to accelerate the process. After this time, no BDT remained, and TLC showed that the resultant material coeluted with an authentic sample of **9**, prepared by treatment of BDT **6a** with dilute aqueous sodium hydroxide (Scheme 1).

BDT in Solution; Studies on Equilibrium Dynamics. Having a convenient method for estimating the BDT [keto **6a**]:[enol **6b**] ratio in solution, we investigated one example of the keto ⇆ enol equilibrium dynamics, approaching from both low and high initial keto content. Starting from a weakly acidified *o*-dichlorobenzene solution (30% enol) and adding 1% EtOAc (final concentration, 2.9×10^{-5} mol L^{-1}), the increasing enol content was monitored from the change in the visible absorbance at 438 nm over time at 25 °C. The final enol content was 54% ($K = 1.16$) at equilibrium, which was reached after 165 min under these conditions. A plot of $-\ln([\text{keto}]_t - [\text{keto}]_{eqm})$ versus time gave a straight line showing gradient $= k_1 + k_{-1} = 3.2 \times 10^{-4}\ s^{-1}$, with $r^2 = 0.999$.[32] From this, k_1 and k_{-1} for the keto ⇆ enol process were calculated to be $k_1 = 1.7 \times 10^{-4}\ s^{-1}$ and $k_{-1} = 1.5 \times 10^{-4}\ s^{-1}$. Starting from a weakly acidified, concentrated ethyl acetate solution (87% enol) and diluting to an identical final solvent mixture of 1% EtOAc/99% *o*-dichlorobenzene (final concentration, 2.3×10^{-5} mol L^{-1}), the final enol content was 51% ($K = 1.06$) at equilibrium, reached after 115 min. A plot of $-\ln([\text{enol}]_t - [\text{enol}]_{eqm})$ versus time again gave a straight line with gradient $= k_1 + k_{-1} = 4.1 \times 10^{-4}\ s^{-1}$, with $r^2 = 0.981$. In this case, k_1 and k_{-1} for the keto ⇆ enol process were calculated to be $k_1 = 2.1 \times 10^{-4}\ s^{-1}$ and $k_{-1} = 2.0 \times 10^{-4}\ s^{-1}$. Results for the final equilibrium constant and forward and reverse rate constants were comparable when approaching the equilibrium from either high or low keto concentration. Clearly these kinetic data are specific to this studied solvent system and the absolute values would be different for others, but nonetheless the observations demonstrate that the keto ⇆ enol equilibrium is fully dynamic, obeying first-order equilibrium kinetics and show that the enol is thermodynamically stable, since its concentration increases on addition of ethyl acetate to the *o*-dichlorobenzene solution, which favors this tautomeric form.

BDT in Solution; Keto−Enol Ratio and Empirical Solvent Properties. Both the NMR and UV−vis data suggest that higher enol-quinonoid content is found in H-bond acceptor (HBA) or basic solvents and predominantly keto-benzenoid content in less or non-HBA solvents. This relationship was explored further by relating the equilibrium constant K defined as $K = [\text{enol}]/[\text{keto}] = [\mathbf{6b}]/[\mathbf{6a}]$ to empirical measures of solvent properties. The Kamlet−Taft solvatochromic scales of solvent dipolarity/polarizability (π^*), H-bond donor strength (α), and H-bond acceptor strength (β) have been widely exploited to investigate many aspects of solvent-based phenomena.[33] In the current context we chose the β_{OH} values recommended in the *Critical Compilation of Scales of Solvent Parameters* of Abboud and Notario,[34] augmented by a few other β values from standard compilations.[35] In fact it was found that the Gibbs energy difference $\Delta G = -2.303RT \log_{10} K$ gave a satisfactory linear correlation with solvent HBA strength (or H-bond basicity) as shown in Figure 8. Inclusion of any of the other Kamlet−Taft parameters in a multilinear treatment was statistically insignificant. Thus, stronger solvent bases interact more favorably with, and stabilize, the relatively acidic enolic OH group of **6b** resulting in a displacement of the equilibrium toward the enol, i.e., **6d** (Figure 8). Extrapolation of the relationship shown in Figure 8 to the gas-phase H-bond basicity of $\beta = 0$ predicts a ΔG of about 5.9 kJ mol^{-1}, suggesting that in the absence of HBA solvent stabilization the keto-tautomer **6a** is favored to the extent [keto]:[enol] = ca. 90:10. This value will be related to calculated relative energies of keto- and enol-tautomers in the following section. Data for solvents in which BDT fully ionizes to give **6c** (DMSO, DMF, etc.) could not be included since it was impossible to acidify the solutions sufficiently to obtain the fully protonated enolic form. The four weakest HBA solvents in the series (chloroform, toluene, chlorobenzene, and *o*-dichlorobenzene) were not included in the determination of the least-squares trend line shown in Figure 8. In all of these the BDT tautomer ΔG differences are approximately the same, and the observed ratios fall somewhat below this line by up to 5 kJ mol^{-1}, indicating the enol-tautomer **6b** is more stabilized in these solvents than expected. In the absence of external H-bond stabilization of the enol by solvent, the enol could adopt a conformation where the enolic OH group now becomes syn to the adjacent lactone carbonyl and in effect is stabilized by an intramolecular five-membered ring "H-bond" (as depicted in conformer **6e**)[36] or favorable dipole−dipole interaction. An alternative source of stabilization could be intermolecular solute OH to solute lactone carbonyl H-bonding, as observed in the solid phase (Figure 4b). The highest observed stabilization is about −13 kJ mol^{-1}, for 2-propanol acting as a HBA base, which is within the range typical for a normal H-bond energy.[37] The H-bond donor solvents (H-bond acids) 2-propanol and acetic acid do not deviate from the trend shown in Figure 8. Any interaction they have with BDT based on their H-bond *donor* ability is clearly having no observable effect on the keto−enol equilibrium.

Structural Dependence of BDT Enolization. We believe that BDT is the first species for which enolization across a benzene ring has been demonstrated. Given that the aromatic resonance stabilization of benzene is considered to be around 135 kJ mol^{-1},[38] the immediate reaction to this observation is that the stabilization energy associated with the central benzene ring of keto-BDT **6a** is being lost on enolization and must in some way be compensated for by the energetics of the enol-tautomer **6b**. Thus, the question of interest is, where is this stabilization coming from to make BDT such a unique species? Various structural features have been considered and explored further with the aid of density

(32) Connors, K. A. In *Chemical Kinetics, the Study of Reaction Rates in Solution*, Wiley-VCH: Weinheim, 1990.
(33) Abboud, J.-L. M.; Kamlet, M. J.; Taft, R. W. In *Progress in Physical Organic Chemistry*; Taft, R. W., Ed.; Interscience-Wiley: New York, 1981; Vol. 13, pp 485−630.
(34) Abboud, J.-L. M.; Notario, R. *Pure Appl. Chem.* **1999**, *71*, 645–718.
(35) (a) Marcus, Y. *Chem. Soc. Rev.* **1993**, *22*, 409–416. (b) Abraham, M. H.; Buist, G. J.; Grellier, P. L.; McGill, R. A.; Prior, D. V.; Oliver, S.; Turner, E.; Morris, J. J.; Taylor, P. J.; Nicolet, P.; Maria, P.-C.; Gal, J.-F.; Abboud, J.-L. M.; Doherty, R. M.; Kamlet, M. J.; Shuely, W. J.; Taft, R. W. *J. Phys. Org. Chem.* **1989**, *2*, 540–552.
(36) Bouchoux, G.; Hoppilliard, Y.; Houriet, R. *Nouv. J. Chim.* **1987**, *11*, 225–233.
(37) Reichardt, C. In *Solvents and Solvent Effects in Organic Chemistry*, 3rd ed.; Wiley-VCH: Weinheim, 2003; p 16.
(38) (a) Schleyer, P. v. R.; Pühlhofer, F. *Org. Lett.* **2002**, *4*, 2873–2876. (b) Howard, S. T. *Phys. Chem. Chem. Phys.* **2003**, *5*, 3113–3119. (c) For a discussion of the energetic aspects of cyclic π-electron delocalization, see: Cyrañski, M. K. *Chem. Rev.* **2005**, *105*, 3773–3811.

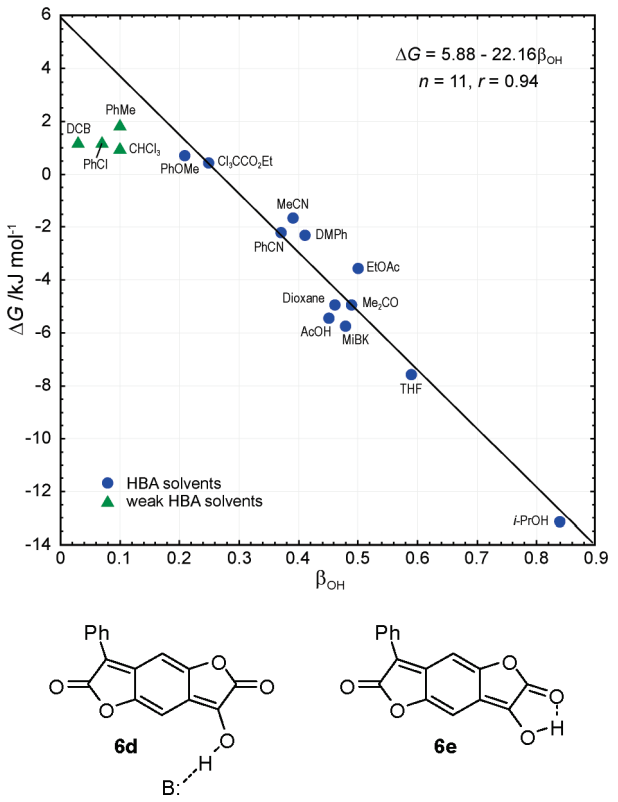

FIGURE 8. Plot of Gibbs energy difference between enol **6b** and keto **6a** tautomers of BDT against the solvent HBA parameter β_{OH} and two proposed solvent-dependent H-bonding systems, **6d** and **6e**.

functional calculations using the GAUSSIAN 03 suite of programs.[39] Gas phase geometries were optimized using a range of basis sets and solvent effects were included within a reaction field using the polarizable continuum model (PCM) and a number of solvents. Solution-phase geometries were also obtained using the PCM approach. The B3LYP exchange-correlation functional was used throughout.

We have discussed already that intermolecular H-bonding is present with appropriate solvents and that the energetics involved are sufficient to drive the equilibrium predominantly toward the enol-tautomer, but even in the absence of H-bonding, the keto-tautomer is extrapolated from Figure 8 to be barely favored (ΔG ca. 5.9 kJ mol^{-1}). The bulk of the enol stabilization must, therefore, derive from elsewhere.

The energy-minimized gas-phase geometries of keto-benzenoid-BDT **6a** and enol-quinonoid-BDT **6b** were calculated and are shown in Figure 9. Two energy minima were found for enol **6b**. First, in the higher energy minimum, the exocyclic enolic OH is oriented away from the adjacent carbonyl group (**6b-anti**). It has geometry close to that determined in the solid phase, except that the torsion about the phenyl-lactone bond is now 31° rather than the 13° and 25° found for the two independent molecules in the asymmetric unit in the crystal (Figure 4a). This value is, however, close to that found in an X-ray structure determination for a benzodifuranone dye.[40] The gas-phase difference in energy between **6a** and **6b-anti** at the 6-311G(2d,p) level is 14.7 kJ mol^{-1} in favor of the keto-tautomer (**6a**). Relative Gibbs energies calculated at 298 K, including zero point energies, solvent plus cavitation, dispersion, and repulsion terms, lowers the $\Delta G(298)$ values to 1.6, 6.6, and 5.3 kJ mol^{-1} for acetonitrile, chlorobenzene and THF, respectively, still in favor of the keto-tautomer. Looking at the individual terms that make up the difference between the gas phase and PCM results in acetonitrile, we found that the main contribution is the preferred stabilization of **6b-anti** by the reaction field solvent model, amounting to 13.1 kJ mol^{-1} preferential lowering of **6b-anti** compared to **6a**. The contributions arising from cavitation, dispersion, and repulsion are very similar in **6a** and **6b-anti** and so largely cancel out, as do the thermal corrections that convert ΔE to $\Delta G(298)$. Second, a slightly lower enol energy minimum was found which corresponds to a geometry in which the hydroxyl O−H bond is oriented syn to the adjacent carbonyl (denoted **6b-syn**). Repeating the comparison for **6b-syn** (see Tables 4 and 5), we find that the quinoidal enol form is now calculated to be the preferred form in the gas and solvent phases. Furthermore, the calculated preference for syn geometry in the gas phase lends support to the conclusion, above, that in non-H-bond donor solvents the enolic tautomer is energetically more favored than the extrapolation from H-bonding solvents would suggest, due to a stabilizing intramolecular H-bond. Overall the calculated energetics of the tautomers of BDT do not differ substantially from those deduced from the solvent studies discussed above. The keto and enol forms are of similar energy in the absence of stronger H-bond donor solvents.

The effect of delocalization of the conjugated extended quinone electronic system into the pendant phenyl ring was determined to be 15.9 kJ mol^{-1} (6-311G(2d,p)) by recalculation of enol **6b** with enforced phenyl ring orthogonality. There is no obvious phenyl interaction in the keto-tautomer **6a**, where the energy-minimized geometry approaches a 90° torsion about the phenyl-lactone bond, so this delocalization must contribute to the overall enol stabilization.

The theoretical calculations were used to explore the aromaticity within the systems of interest. In particular the nucleus independent chemical shift (NICS) index of aromaticity was calculated for each of the rings comprising both tautomers **6a** and **6b**. The NICS index reflects the nature of the ring current induced by an external magnetic field, where a negative NICS value implies a diatropic ring current, and aromaticity for that ring.[41] We report here NICS(0) values, obtained at the centroid of each ring. Since the four rings in **6a** and **6b** are not coplanar, it is not straightforward to define NICS(1) centers (i.e., 1 Å above the molecular plane).

(39) *Gaussian 03, Revision C.02*, Frisch, M. J.; Trucks, G. W.; Schlegel, H. B.; Scuseria, G. E.; Robb, M. A.; Cheeseman, J. R.; Montgomery, Jr., J. A.; Vreven, T.; Kudin, K. N.; Burant, J. C.; Millam, J. M.; Iyengar, S. S.; Tomasi, J.; Barone, V.; Mennucci, B.; Cossi, M.; Scalmani, G.; Rega, N.; Petersson, G. A.; Nakatsuji, H.; Hada, M.; Ehara, M.; Toyota, K.; Fukuda, R.; Hasegawa, J.; Ishida, M.; Nakajima, T.; Honda, Y.; Kitao, O.; Nakai, H.; Klene, M.; Li, X.; Knox, J. E.; Hratchian, H. P.; Cross, J. B.; Bakken, V.; Adamo, C.; Jaramillo, J.; Gomperts, R.; Stratmann, R. E.; Yazyev, O.; Austin, A. J.; Cammi, R.; Pomelli, C.; Ochterski, J. W.; Ayala, P. Y.; Morokuma, K.; Voth, G. A.; Salvador, P.; Dannenberg, J. J.; Zakrzewski, V. G.; Dapprich, S.; Daniels, A. D.; Strain, M. C.; Farkas, O.; Malick, D. K.; Rabuck, A. D.; Raghavachari, K.; Foresman, J. B.; Ortiz, J. V.; Cui, Q.; Baboul, A. G.; Clifford, S.; Cioslowski, J.; Stefanov, B. B.; Liu, G.; Liashenko, A.; Piskorz, P.; Komaromi, I.; Martin, R. L.; Fox, D. J.; Keith, T.; Al-Laham, M. A.; Peng, C. Y.; Nanayakkara, A.; Challacombe, M.; Gill, P. M. W.; Johnson, B.; Chen, W.; Wong, M. W.; Gonzalez, C.; Pople, J. A. Gaussian, Inc.: Wallingford, CT, 2004.

(40) Malone, J. F; Bullock, J. F. Personal communication.

(41) Chen, Z.; Wannere, C. S.; Corminboeuf, C.; Puchta, R.; Schleyer, P. v. R. *Chem. Rev.* **2005**, *105*, 3842–3888.

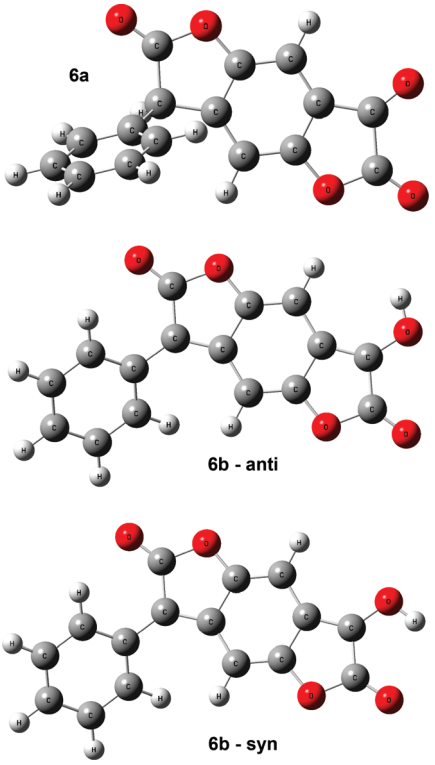

FIGURE 9. Calculated energy-minimized [6-311G(2d,p)] gas-phase geometries of keto-BDT **6a**, enol-BDT **6b-anti**, and enol-BDT **6b-syn**.

Furthermore, we are concerned here with the change in the NICS values rather than the absolute values themselves, and so the NICS(0) values should be adequate.

The results are shown in Table 6. As expected, the pendant phenyl ring D (as defined in Table 6) retains its aromaticity for both tautomers. The central six-membered ring B is aromatic in the keto-tautomer (NICS(0) = −7.5) but loses this aromaticity on enolization (NICS(0) = −0.4). This again is expected on the basis of the conventional structural representations for the two tautomers and lies at the heart of our interest in the energetic basis for the ease of enolization of BDT. The phenyl-substituted lactone ring A has a NICS(0) value of +0.8 in the keto-tautomer and −1.3 in the enol, implying at best a weak or negligible tendency to aromatization on enolization. The result for ring C in BDT is more surprising. In the keto-tautomer its NICS(0) value of +7.2 indicates an unexpected and significant *anti* aromaticity. This result is by no means intuitive. Moreover, the NICS(0) value of −2.1 in the enol implies aromatization or, more significantly, the removal of the antiaromatic character in **6a**. The tempting qualitative inference is that the loss of aromaticity and corresponding decreased stabilization energy associated with the central ring B is more or less compensated by removal of the antiaromatic destabilization of ring C as it enolizes. To quantify this effect, we would like to be able to relate the NICS changes to aromatic stabilization energies (ASE). While a reasonable correlation between NICS and ASE has been shown for a set of more than 100 heteroaromatic ring systems, we note the warning that

(42) Cyrański, M. K.; Krygowski, T. M.; Katritzky, A. R.; Schleyer, P. v. R. *J. Org. Chem.* **2002**, *67*, 1333–1338.

TABLE 4. Relative Energies (kJ mol^{-1}) in the Gas Phase and PCM Solvent Model with Different Basis Sets Using the B3LYP Functional

	E(**6b-anti**) − *E*(**6a**)		*E*(**6b-syn**) − *E*(**6a**)	
phase/basis set	6-31G(d,p)	6-311G(2d,p)	6-311G+(2d,p)	6-311G(2d,p)
gas	20.9	14.7	14.4	−4.9
acetonitrile	7.3	1.6		−3.5
chlorobenzene	12.2	6.6		−2.7
THF	10.8	5.3		−2.9

TABLE 5. Relative Free Energies at 298 K (kJ mol^{-1}) Including Zero Point Energies in the Gas Phase and PCM Solvent Model with Different Basis Sets Using the B3LYP Functional

	G(**6b-anti**) − *G*(**6a**)		*G*(**6b-syn**) − *G*(**6a**)
phase/basis set	6-31G(d,p)	6-311G(2d,p)	6-311G(2d,p)
gas	27.5		
acetonitrile	3.3	5.0	−6.4
chlorobenzene	11.7	11.3	−5.0
THF	10.5	8.2	−5.4

TABLE 6. NICS Values[a] for the Four Rings within Keto-BDT 6a and Enol-BDT 6b

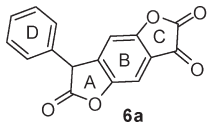

6a

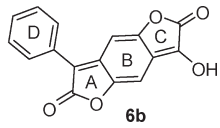

6b

	ring			
	A	B	C	D
keto-BDT (**6a**)	+0.8	−7.5	+7.2	−8.3
enol-BDT (**6b**)	−1.3	−0.4	−2.1	−7.3
difference on enolization[a]	−2.1	+7.1	−9.3	+1.0

[a]Negative values correspond to aromaticity; positive values to antiaromaticity. [b]Negative differences correspond to stabilization on enolization.[41]

"energetic... and magnetic descriptors of aromaticity... do not speak with the same voice"[42] and in the absence of stronger justification, regrettably conclude that translation of the NICS values into ASE for BDT is currently unwarranted.[43] However, we do feel that removal of the antiaromatic destabilization of ring C is a surprising, feasible, and at least contributory explanation for the relative ease of phenylogous enolization for this molecule.

Literature precedent for antiaromaticity in α-dicarbonyl heterocycle systems analogous to BDT appears to be limited to a single study of the nitrogen analogue isatin **11**.[44] Thermochemical considerations allowed construction of the isodesmic reaction connecting isatin with *o*-xylene as in Figure 10. This reaction was estimated to be exothermic by 38 kJ mol^{-1}, leading to the conclusion that isatin is appreciably antiaromatic. Since the heterocycle in isatin is isoelectronic with the keto-lactone ring C of keto-BDT, it seems fair to conclude that the antiaromaticity of this ring already

(43) More recent studies continue to develop links between energetic and magnetic criteria of aromaticity, as for example circuit resonance energies of polycyclic aromatic hydrocarbons. Aihara, J.-i. *J. Am. Chem. Soc.* **2006**, *128*, 2873–2879.

(44) (a) Matos, M. A. R.; Miranda, M. S.; Morais, V. M. F.; Liebman, J. F. *Org. Biomol. Chem.* **2003**, *1*, 2566–2571. (b) Matos, M. A. R.; Liebman, J. F. *Top. Heterocycl. Chem.* **2009**, *19*, 1–26.

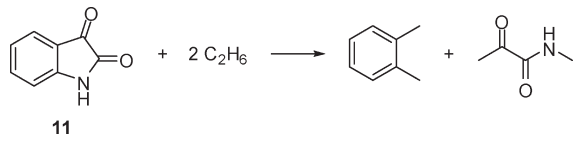

FIGURE 10. Isodesmic reaction connecting isatin (**11**) with *o*-xylene.[44]

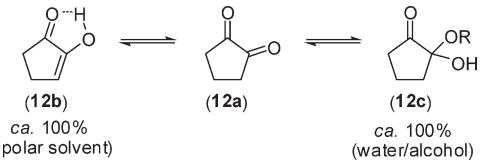

FIGURE 11. Reported equilibrium constitution of 1,2-cyclopentanedione **12** in aprotic and aqueous/alcoholic media.[45,47]

indicated by the NICS calculations should also be reflected by an appreciable thermochemical aromatic destabilization energy. Again, we demur from giving it a value.

As well as consideration of the antiaromatic destabilization in α-keto-lactone ring C, small (less than seven-membered) alicyclic 1,2-dicarbonyl systems, for example, 1,2-cyclopentanedione[45] **12a** (Figure 11) and dihydrofuran-2,3-dione,[46] are known to exist exclusively as their enol-tautomers, i.e., **12b**, in aprotic, non-H-bonding solvents. In such rings, the locked *s-cis* conformation of the carbonyl groups enforces an unfavorable dipole−dipole interaction, which destabilizes the diketo-tautomer **12a**.[3f] Additionally, the enol-tautomer can be further stabilized by an intramolecular hydrogen bond,[36] a phenomenon that may occur for BDT in weak HBA solvents, as discussed previously. However, in aqueous or alcoholic media, the enol content of 1,2-cyclopentanedione is low, resulting from preferable formation of the ketone-hydrate/hemiacetal **12c**.[47] Interestingly, in nonscrupulously dried water-miscible solvents, BDT still equilibrates to the enol-tautomer **6b** at the expense of aromatic stabilization instead of forming an alternative benzenoid-ketone-hydrate, which would presumably also remove antiaromaticity. However, in BDT, the resultant enolic−OH is delocalized into an extended π-system, whereas in 1,2-cyclopentanedione **12b** only resonance into a single double bond exists.

In summary, there are several factors that contribute to the energetics of the enolization of BDT, not all of which can yet be quantified. The main drivers are (a) destabilizing antiaromaticity of the keto-lactone ring of **6a**, removed in enol-tautomer **6b**; (b) further stabilizing π-electron delocalization in the extended conjugated ring system of **6b**; (c) relaxation of the destabilizing *syn*-1,2-dicarbonyl dipole−dipole interaction in the keto-lactone ring; and (d) the pendant phenyl ring of BDT, which contributes stabilization to the enol-tautomer **6b** by π-overlap effects, judging by the detrimental effect of removing its coplanarity. In addition to these, H-bond acceptor solvents give intermolecular stabilization of the enol **6b** through H-bonding to the enolic OH group, and result in keto-tautomer **6a** giving way to almost total enol **6b** content in a strong H-bond acceptor like 2-propanol.

TABLE 7. Comparion of ^{13}C NMR Shifts (DMSO-d_6 + Et_3N) for BDT Enolate 6c and Enol-Ether 7

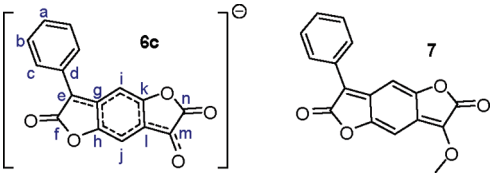

carbon	$\delta_{(ppm)}$ enolate **6c**	$\delta_{(ppm)}$ enol-ether **7**	$\delta_{(ppm)}$ difference
a	124.7	129.6	−4.9
b	128.3	129.0	−1.6
c	125.8	128.6	−2.8
d	134.4	129.4	+5.0
e	97.4	120.1	−22.7
f	169.4	168.0	+1.4
g	144.1	138.7	+5.4
h	142.6	153.5	−10.9
i	92.0	98.0	−6.0
j	98.5	98.0	+0.5
k	166.3	149.8	+16.5
l	107.2	116.6	−9.4
m	159.9	145.1	+14.8
n	163.5	162.2	+1.2

BDT Enolate. In strongly H-bonding and high relative permittivity solvents with β values >0.6 such as DMF, DMA, DMSO etc., complete ionization of BDT occurred resulting in liberation of the intensely purple-colored free enolate anion **6c** with an intense broad absorption at λ_{max} 550−555 nm with a bathochromic shoulder and ε_{max} of 35,000 (Figure 7). No absorption was seen for the enol-tautomer at ca. 440 nm in these solvents, even on addition of MSA. The ionization is presumably stabilized by a combination of favorable proton solvation by the basic solvent and dielectric stabilization of the ions due to the high relative permittivities of these solvents. Tertiary amines like triethylamine and pyridine also ionized BDT, either as neat solution or on their addition to BDT in other solvents, presumably because of their strong basicity and proton solvation. The addition of triethylamine to a DMSO or DMF solution gave no change in the observed λ_{max} or ε_{max}, indicating further that BDT already existed fully ionized in these solvents.

The nature of the enolate was studied by NMR spectroscopy. BDT enolate **6c** in deuterated DMSO (containing a small amount of triethylamine to further sharpen the spectrum) showed a single entity strongly resembling the enol-tautomer. The ^{1}H spectrum displayed the characteristic high field central ring proton resonances at δ 6.80 and δ 6.82 ppm and low field resonances for the 7-phenyl *ortho*-protons at δ 7.83 ppm. The ^{13}C NMR spectrum of **6c** was fully assigned with the assistance of HMQC and HMBC analysis. When compared to ^{13}C data for the enol-ether **7** (Table 7), this gave a qualitative insight into where negative charge was localized on deprotonation, from the difference in chemical shifts. The comparison is made here to the enol-ether **7** rather than directly to the enol **6b**, since the ^{13}C NMR spectrum of the enol-ether was fully assigned by HMQC/HMBC experiments, and that of the enol **6b** was itself made by comparison to the enol-ether **7**. Of particular interest are carbons C_e and C_m (as defined in Table 7). The downfield

(45) Cumper, C. W. N.; Leton, G. B.; Vogel, A. I. *J. Chem. Soc.* **1965**, 2067–2072.

(46) (a) Wasserman, H. H.; Ives, J. L. *J. Org. Chem.* **1978**, *43*, 3238–3240. (b) Schank, K.; Beck, H.; Pistorius, S. *Helv. Chim. Acta* **2004**, *87*, 2025–2049. Blank, I.; Lin, J.; Fumeaux, R.; Welti, D. H.; Fay, L. B. *J. Agric. Food Chem.* **1996**, *44*, 1851–1856.

(47) Bakule, R.; Long, F. A. *J. Am. Chem. Soc.* **1963**, *85*, 2309–2312.

chemical shift for C_m (δ 159.9 ppm) relative to the enol-ether (δ 145.1 ppm) indicates a higher degree of ketone character at this position in the enolate, tending toward the shift seen in the fully keto tautomer **6a** (δ 178.8 ppm). However, despite the increasing ketone character at C_m, the shift of the lactone carbonyl C_n is largely unaffected, suggesting that the C ring in the enolate has none of the antiaromatic character seen in the keto-tautomer. Carbon C_e is significantly more shielded in the enolate (δ 97.4 ppm) compared to the enol-ether (δ 120.1 ppm). Similarly, smaller increases in electron density are identified at C_i and weakly in the *exo*-phenyl ring at C_a and C_c, which are intuitive from consideration of standard resonance canonical forms. Carbons C_g and C_k in the central ring also show large differences compared to the enol, tending closer to the shifts seen for these carbons in the keto-standard **8** (δ 138.9, δ 161.7 ppm, respectively), suggesting greater aromatic character in the central ring on deprotonation. Lactone carbon C_f shows little change in the enolate, indicating little delocalization of charge into this position.

Comparison of data, therefore, indicates that the negative charge in the enolate is not fully localized on oxygen, but that the enolate exists part-way between an enol-like and keto-like structure, with the bulk of the negative charge split between the keto/enol-oxygen and the benzylic carbon C_e.

Conclusions

The first example of a stable phenylogous enol has been isolated, and its structure was proven by X-ray crystallography. The equilibrium between the keto- and enol-tautomers was quantified in solution, and the position of equilibrium showed a linear correlation to the Kamlet−Taft solvatochromic scale for solvent H-bond acceptor strength (β_{OH}). We attribute the surprising apparent net stabilizing effect on enolization despite the loss of the aromatic resonance stabilization of the central benzene ring to several energetically favorable outcomes including a loss of destabilizing antiaromaticity of the keto-lactone ring of **6a** that is not present in enol-tautomer **6b**, increased π-electron delocalization in the enol extended conjugated ring system, removal of the destabilizing *syn*-1,2-dicarbonyl dipole−dipole interaction present in the keto-lactone ring of **6a**, and π-overlap of the pendant phenyl ring in the enol-tautomer **6b**. In solution, H-bond acceptor solvents gave further intermolecular stabilization of the enol **6b** through H-bonding to the enolic OH group, leading to measurable differences in the observed equilibrium position. In strongly H-bonding and high relative permittivity solvents with β values >0.6 BDT existed exclusively as the free enolate anion **6c**, part-way between an enol-like and keto-like structure.

Experimental Section

Exemplary ^{1}H and ^{13}C data are supplied here. The behavior of all compounds was studied in numerous solvents. Further details and spectral assignments are available in Supporting Information.

7-Phenyl-7*H*-benzo[1,2-b;4,5-b′]difuran-2,3,6-trione (BDT; 6a). Prepared according to ref 19. UV−vis see Table 3; FTIR (KBr cm^{-1}; exists as H-bonded enol **6b**) ν_{max} 1782 (lactone C=O), 1692 (H-bonded lactone C=O), 1623, 1579; δ_H (400 MHz, DMSO-d_6; exists as enolate **6c**) 6.80 (1H, s), 6.82 (1H, s), 7.15 (1H, tt, J = 1.2, J = 7.0), 7.37 (2H, m), 7.82 (2H, dd, J = 1.2, J = 8.3); δ_C (100 MHz, DMSO-d_6 + Et_3N; exists as enolate **6c**) 8.9, 45.8, 92.0, 97.4, 98.5, 107.2, 124.7, 125.8, 128.3, 134.4, 142.6, 144.1, 159.9, 163.5, 166.3, 169.4. m/z (CI+) 284 (100%), 298 (25%, M + NH_4^+). Anal. Calcd for $C_{16}H_8O_5$: C, 68.58; H, 2.88. Found: C, 68.64; H, 2.80.

3-Methoxy-7-phenyl-7*H*-benzo[1,2-b;4,5-b′]difuran-2,6-dione (7). 7-Phenyl-7*H*-benzo[1,2-b;4,5-b′]difuran-2,3,6-trione (**6a**) (2.8 g, 10 mmol) was suspended in toluene (100 mL). At rt a solution of trimethylsilyl-diazomethane (2 M, 6 mL, 12 mmol) was added dropwise over ca. 1 min. Gas evolution was seen immediately, and the suspended solid turned from a dark purple to a yellow-brown color. The suspension was stirred overnight. The solid was then filtered off, washed with further toluene, and dried overnight in a fan oven at 40 °C (mass = 2.25 g). The material was recrystallized from a large volume of boiling methyl isobutyl ketone, to obtain analytically pure material (1.78 g, 60%) as fine orange-brown needles: UV−vis see Table 1; FTIR (KBr cm^{-1}) ν_{max} 1785 (lactone C=O), 1753 (lactone C=O), 1620, 1583, 1369; δ_H (400 MHz, DMSO-d_6) 4.31 (3H, s), 7.13 (1H, s), 7.29 (1H, s), 7.45−7.55 (3H, m), 7.79 (2H, m); δ_C (100 MHz, DMSO-d_6) 60.8, 97.97, 98.00, 116.6, 120.1, 128.6, 129.0, 129.4, 129.6, 138.7, 145.1, 149.8, 153.5, 162.2, 168.0. m/z (APCI+) 295 (100%, M + H^+). Anal. Calcd for $C_{17}H_{10}O_5$: C, 69.39; H, 3.43. Found: C, 69.45; H, 3.28.

Methyl 2-(5-Hydroxy-2-oxo-3-phenyl-2,3-dihydrobenzofuran-6-yl)-2-oxoacetate (8). 7-Phenyl-7*H*-benzo[1,2-b;4,5-b′]difuran-2,3,6-trione (**6a**) (1.5 g, 5.34 mmol) was suspended in methanol (60 mL), heated to boiling to effect a fine suspension, and then allowed to stir overnight at ambient temperature. Residual trace suspended solid was filtered off, and the solvent was evaporated under reduced pressure. A small amount (ca. 5 mL) of methanol was added to redissolve the resulting purple oily solid, and the solution was allowed to stand overnight. The required product was filtered off, washed with a small portion of ice-cold methanol (20 mL), pulled dry under vacuum, and dried in a fan oven at 40 °C overnight to give **8** (0.74 g, 45%) as a yellow solid: UV−vis (CH_2Cl_2 + trace CH_3SO_3H) λ_{max} 368 nm, ε_{max} 4,250; FTIR (KBr cm^{-1}) ν_{max} 1791 (lactone), 1741 (ester), 1624 (H-bonded ketone); FTIR (CH_2Cl_2 cm^{-1}) ν_{max} 1819, 1744, 1644 and 1583; δ_H (400 MHz, $CDCl_3$) 4.03 (3H, s), 4.95 (1H, d, J = 0.7), 6.91 (1H, d, J = 1.0), 7.20 (2H, m), 7.33−7.44 (3H, m), 7.57 (1H, s), 11.35 (1H, s). δ_C (100 MHz, $CDCl_3$) 50.1, 53.3, 111.8, 115.2, 115.8, 128.1, 128.6, 129.3, 133.5, 138.9, 146.1, 161.7, 162.1, 173.5, 189.1. m/z (CI+) 136 (100%), 262 (80%), 330 (15%, M + NH_4^+). Anal. Calcd for $C_{17}H_{12}O_6$: C, 65.39; H, 3.87. Found: C, 65.41; H, 3.77.

2-(5-Hydroxy-2-oxo-3-phenyl-2,3-dihydrobenzofuran-6-yl)-2-oxoacetic Acid (9). 7-Phenyl-7*H*-benzo[1,2-b;4,5-b′]difuran-2,3,6-trione (**6a**) (2.7 g, 9.64 mmol) was suspended in 0.1 N $NaOH_{(aq)}$ (200 mL) and stirred at ambient temperature for 30 min, after which time the solid had dissolved. The solution was screened through a glass fiber filter to remove residual traces of insoluble materials and then adjusted to pH 2 by dropwise addition of 2 N $HCl_{(aq)}$. Sodium chloride (30 g) was added and stirred for 2 h to aid precipitation of the required product. The product was filtered off, washed with a small volume of ice-cold water, and then dried in a fan oven at 40 °C overnight to yield a pale brown solid (2.1 g, 73%), which was >99% organically pure by ^{1}H NMR. To obtain analytically pure material, a portion of the obtained solid was recrystallized from boiling methylated spirit: UV−vis (acetone + trace CH_3SO_3H) λ_{max} 357 nm, ε_{max} 4,050; FTIR (CH_2Cl_2 cm^{-1}) ν_{max} 1817 (lactone), 1779, 1758, 1649, 1621, 1580; δ_H (400 MHz, $CDCl_3$) 4.95 (1H, br. s), 6.96 (1H, d, J = 1.0), 7.22 (2H, m), 7.37−7.44 (3H, m), 8.25 (1H, s), 11.39 (1H, br. s). δ_C (100 MHz, $CDCl_3$) 50.4, 112.5, 115.2, 115.9, 128.2, 128.8, 129.5, 133.4, 139.7, 146.3, 161.5, 162.5, 173.9, 187.4. m/z (ES−) 297 (100%, [M − H^+]$^-$). Anal.

Calcd for $C_{16}H_{10}O_6 \cdot 0.45$ NaCl: C, 59.21; H, 3.11. Found: C, 59.21; H, 2.98.

Acknowledgment. We are grateful to the following people who are or were based at The University of Manchester, School of Chemistry: M. Chem. students Khalid Ali, Simon McCormack, and Collette Turner for their experimental input; Drs. Ian Watt and Peter Quayle for invaluable discussion; and staff in the NMR department, especially Mr Stephen Kelly, for their assistance in obtaining data.

Supporting Information Available: General experimental information. Assigned ^{1}H, ^{13}C, HMQC, and HMBC spectra for all compounds measured in a range of solvents. X-ray crystallographic data for **6b** in CIF format. Details on solution-phase equilibrium dynamics measurements for **6a**/**6b**. Further discussion on the UV−vis spectrum of keto-BDT **6a**. Confirmation of a linear relationship between A and concentration for enol-BDT in UV−vis measurements. Gas-phase Cartesian coordinates for **6a**/**6b** from energy minima calculations. This material is available free of charge via the Internet at http://pubs.acs.org.